physica status solidi a
www.pss-a.com
applications and materials science

Characterization of Fe 3d states in $CuFeS_2$ by resonant X-ray emission spectroscopy

Katsuaki Sato[1,2], Yoshihisa Harada[3,4,5], Munetaka Taguchi[4], Shik Shin[4,5,6], and Atsushi Fujimori[7]

[1] Graduate School of Engineering, Tokyo University of Agriculture and Technology, Nakacho, Koganei, Tokyo 184-8588, Japan
[2] Office of Basic Research, Japan Science and Technology Agency (JST), Sambancho, Chiyoda-ku, Tokyo 102-0075, Japan
[3] Department of Applied Chemistry, The University of Tokyo, 7-3-1 Hongo, Bunkyo-ku, Tokyo 113-8656, Japan
[4] RIKEN/SPring-8, 1-1-1 Kouto, Sayo-cho, Sayo-gun, Hyogo 679-5148, Japan
[5] CREST, Japan Science and Technology Agency (JST), 4-1-8 Hon-cho, Kawaguchi, Saitama 332-0012, Japan
[6] Institute for Solid State Physics (ISSP), The University of Tokyo, 5-1-5, Kashiwanoha, Kashiwa, Chiba 277-8581, Japan
[7] Department of Physics, The University of Tokyo, 7-3-1 Hongo, Bunkyo-ku, Tokyo 113-8656, Japan

Received 2 September 2008, revised 28 October 2008, accepted 1 December 2008
Published online 17 March 2009

PACS 71.20.Nr, 75.10.Dg, 75.50.Ee, 75.50.Pp, 78.70.En

Resonant X-ray emission spectroscopy (RXES) experiments were carried out in a single crystal of chalcopyrite $CuFeS_2$, an antiferromagnetic semiconductor with a golden lustre, to unravel the overlapping d–d and charge-transfer transitions extending well above the absorption edge, which cannot be observed by conventional optical absorption experiments. The observed RXES spectra have been analyzed by means of cluster-model calculation with configuration interaction, which leads to the conclusion that $CuFeS_2$ is a Haldane–Anderson insulator with a negative value of charge transfer energy, $\Delta = -3$ eV.

Phys. Status Solidi A **206**, No. 5, 1096–1100 (2009) / **DOI** 10.1002/pssa.200881196

Phys. Status Solidi A **206**, No. 5, 1096–1100 (2009) / **DOI** 10.1002/pssa.200881196

physica status solidi a
www.pss-a.com
applications and materials science

Characterization of Fe 3d states in $CuFeS_2$ by resonant X-ray emission spectroscopy

Katsuaki Sato[*,1,2], **Yoshihisa Harada**[3,4,5], **Munetaka Taguchi**[4], **Shik Shin**[4,5,6], **and Atsushi Fujimori**[7]

[1] Graduate School of Engineering, Tokyo University of Agriculture and Technology, Nakacho, Koganei, Tokyo 184-8588, Japan
[2] Office of Basic Research, Japan Science and Technology Agency (JST), Sambancho, Chiyoda-ku, Tokyo 102-0075, Japan
[3] Department of Applied Chemistry, The University of Tokyo, 7-3-1 Hongo, Bunkyo-ku, Tokyo 113-8656, Japan
[4] RIKEN/SPring-8, 1-1-1 Kouto, Sayo-cho, Sayo-gun, Hyogo 679-5148, Japan
[5] CREST, Japan Science and Technology Agency (JST), 4-1-8 Hon-cho, Kawaguchi, Saitama 332-0012, Japan
[6] Institute for Solid State Physics (ISSP), The University of Tokyo, 5-1-5, Kashiwanoha, Kashiwa, Chiba 277-8581, Japan
[7] Department of Physics, The University of Tokyo, 7-3-1 Hongo, Bunkyo-ku, Tokyo 113-8656, Japan

Received 2 September 2008, revised 28 October 2008, accepted 1 December 2008
Published online 17 March 2009

PACS 71.20.Nr, 75.10.Dg, 75.50.Ee, 75.50.Pp, 78.70.En

* Corresponding author: e-mail satokats@cc.tuat.ac.jp

Resonant X-ray emission spectroscopy (RXES) experiments were carried out in a single crystal of chalcopyrite $CuFeS_2$, an antiferromagnetic semiconductor with a golden lustre, to unravel the overlapping d–d and charge-transfer transitions extending well above the absorption edge, which cannot be observed by conventional optical absorption experiments. The observed RXES spectra have been analyzed by means of cluster-model calculation with configuration interaction, which leads to the conclusion that $CuFeS_2$ is a Haldane–Anderson insulator with a negative value of charge transfer energy, $\Delta = -3$ eV.

1 Introduction Chalcopyrite $CuFeS_2$ is a well-known mineral with a golden lustre. It is a semiconductor since it shows a rectifying property [1], a considerably large thermoelectric power [2], and a photoconductivity spectrum with a peak around 0.9 eV [3]. Electrical measurements on a natural single crystal show a typical activation-type temperature dependence of electrical conductivity with an activation-energy of 1.3 eV and a Hall mobility of 35 cm^2/Vs [2]. On the contrary, synthetic $CuFeS_2$ single crystals show an electrical conductivity of typical degenerate semiconductors with a temperature-independent carrier concentration of 4×10^{20} cm^{-3} (undoped n-type) and 5×10^{19} cm^{-3} (Zn-doped p-type) [4].

The neutron diffraction [5] and static magnetic experiments [2] revealed that $CuFeS_2$ is an antiferromagnetic material with Néel temperature of 823 K. According to the neutron studies the effective magnetic moment of Fe and Cu is $3.85\mu_B$ and $0.0 \pm 0.2\mu_B$, respectively. The magnetic moment is considerably reduced from $5\mu_B$, which is expected from the ionic state of $Cu^+Fe^{3+}S_2$. The observed reduction of Fe moment is consistent with the model proposed by Pauling and Brockway, who concluded that chalcopyrite is a mixture of two extreme ionic states, $Cu^+Fe^{3+}S_2$, and $Cu^{2+}Fe^{2+}S_2$ [6]. Mössbauer effect studies at room temperature resulted in a six-line spectrum which indicates that the Fe in $CuFeS_2$ is trivalent and present in ordered states [7, 8]. Schneider et al. observed the electron paramagnetic resonance (ESR) spectrum of Fe^{3+} ions in $CuGaS_2$:Fe [9]. Oxidation states of the metals in $CuFeS_2$ and related materials have been extensively discussed using different X-ray spectroscopy experiments; eg., X-ray absorption near-edge structure (XANES) [10], near-edge X-ray absorption fine structure (NEXAFS) [11], and X-ray photoelectron spectroscopy (XPS) combined with X-ray absorption spectroscopy (XAS) [12]. Nevertheless the oxidation state of $CuFeS_2$ is still a matter of controversy.

Optical absorption spectrum in thin films of $CuFeS_2$ shows a rapid increase of absorption from 0.6 eV, which is associated with the energy gap of 0.5 eV determined by Austin et al. [13]. Optical absorption studies in Fe-doped $CuAlS_2$ and $CuGaS_2$ revealed that strong absorption band with two peaks A (around 1.1 eV) and B (around 1.9 eV)

[3], which develop to the broad band-to-band absorption with a shoulder at 1 eV and a broad peak around 2 eV observed in $CuFeS_2$ [14, 15]. Molecular orbital calculation in 17-atom cluster revealed that d-orbitals are hybridized with p-orbitals of sulphur atoms and located between occupied valence band composed of Cu 3d and S 3p orbitals and unoccupied conduction band comprising of Cu 4s and Fe 4s states [16]. The calculated magnetic moment was estimated as $2.8\mu_B$ for the centre Fe and $-3.7\mu_B$ for the corner Fe in the cluster. The reduction of Fe moment was explained by hybridization of 3d orbitals with ligand orbitals. An energy band calculation was performed using a DV-Xα technique, which gives a band gap value of 0.72 eV and a magnetic moment of $3.88\mu_B$ [17].

A sharp photoluminescence (PL) line with phonon replicas has been observed at quite low energy in slightly Fe-doped $CuGaS_2$ and $CuAlS_2$, i.e., at 4942 cm^{-1} = 0.613 eV for $CuGaS_2$:Fe, and 5804 cm^{-1} = 0.720 eV for $CuAlS_2$:Fe [18]. The theoretical analysis of the six-line-split Zeeman lines in terms of the ligand-field theory leads to an assignment of the infrared PL line as $^4T_1$ to $^6A_1$ transition in the $3d^5$ manifold in Fe^{3+} [18]. It is found from PL studies in $CuAl_xGa_{1-x}S_2$:Fe that the low energy PL line is derived from the Fe-ion occupying the Cu-site [19]. Results of thermal treatment of $CuGaS_2$:Fe in different atmosphere suggest that the infrared PL is originated from the Fe occupying the Cu-site, and the strong absorption bands from the Fe ion at Ga site [20].

It is difficult, however, to interpret the PL line in terms of the ordinary d–d transition in a free Fe^{3+} ion, since all quartet states including the $^4T_1$ state of d^5 configurations are situated at much higher energy region in Tanabe–Sugano diagram [21]. Kambara et al. calculated the electronic states of a tetrahedral cluster composed of a Fe ion and four sulphur ions using the LCAO MO schemes with configuration interactions (CI), in which two absorption peaks were assigned to charge transfer (CT) transitions from the $^6A_1$ ground state to the lowest two $^6T_2$ excited states, while the infrared emission was attributed to the transition from the lowest $^4T_1$ or $^4T_2$ excited states to the $^6A_1$ ground state with the transition energy of 0.707 eV and 0.299 eV, respectively [22]. It is revealed that although the expression of the ground state of Fe is $^6A_1$, the state is composed of not only the $3d^5$ states but also the charge transferred states of $3d^6\underline{L}$, $3d^7\underline{L}^2$, etc., where $\underline{L}$ stands for a ligand hole.

Similar reduction of the d–d transition energy and the existence of multiple charge states of transition-metal impurities in semiconductors have been discussed by Haldane and Anderson by means of the Anderson Hamiltonian [23]. The solution of the Hamiltonian for various values of the parameters describing the problem fall into two regimes, whether the p–d hybridization energy V_{pd} is smaller or larger than the d–d Coulomb energy U. For $V_{pd} < U$, the weak coupling limit, the ground state of the impurity resembles the free atom, and as V_{pd} approaches the transition region $V_{pd} \sim U$, all ten possible charge states of the impurity can be bound in the gap by varying the Fermi level, and finally if $V_{pd} > U$, the strong coupling limit, d-levels in the gap become a degenerate level repelled from the band edge to the gap centre and many-electron effects become negligible. The electronic properties suggest that $CuFeS_2$ is in the intermediate region, i.e., $V_{pd} \sim U$.

Photoelectron spectra of valence band region and Fe 2p core states of $CuFeS_2$ and $CuAlS_2$:Fe were measured with synchrotron radiation and analyzed by a cluster-model configuration-interaction (CI) calculation on the $(FeS_4)^{5-}$ cluster. Optimum values for the CT energy Δ, the d–d Coulomb energy U, and p–d transfer integrals (pdσ) and (pdπ) are determined by fitting the calculated Fe 3d-derived spectrum and the Fe 2p core XPS spectra to the experimental ones. From this analysis the parameters are determined as $\Delta = -0.5 \pm 0.5$ eV, $U = 4.0 \pm 1.0$ eV, and $(pd\sigma) = 1.5 \pm 0.2$ eV [24].

Zaanen et al. discussed the dependence of the conductivity gap and the nature of electron and hole states on U and Δ for transition-metal compounds, and summarized the result in the so-called Zaanen–Sawatzky–Allen diagram [25]. By plotting in the diagram the considerably large U and the negative Δ determined above, it is suggested that $CuFeS_2$ is in the intermediate region, in which there are strong fluctuations between the states d^n, $d^{n+1}\underline{L}$, $d^n\underline{L}$, and d^{n+1}. This leads to a conclusion that $CuFeS_2$ is an unusual insulator of Haldane–Anderson type brought about by strong p–d hybridization.

We therefore consider that 3d sates of Fe in $CuFeS_2$ are strongly hybridized with valence p-orbitals, which makes the ground state not purely $3d^n$, but a mixture of $3d^n$ and charge-transferred states such as $3d^{n+1}\underline{L}$ and $3d^{n+2}\underline{L}^2$. If the CT energy Δ is negative, the d–d multiplets become pushed down from the CT continuum, as illustrated in Fig. 1. In order to get further information on the 3d states of Fe in $CuFeS_2$, resonant X-ray emission spectroscopy (XES) has been carried out. The present paper describes experimental results and theoretical analysis on the resonant XES result.

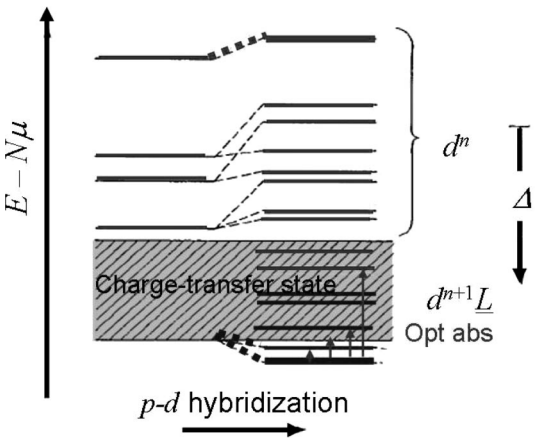

Figure 1 Schematic diagram illustrating 3d electronic states of $CuFeS_2$, in which CT energy is negative and excited $3d^{n+1}\underline{L}$ states ($n = 5$) overlap with the CT state.

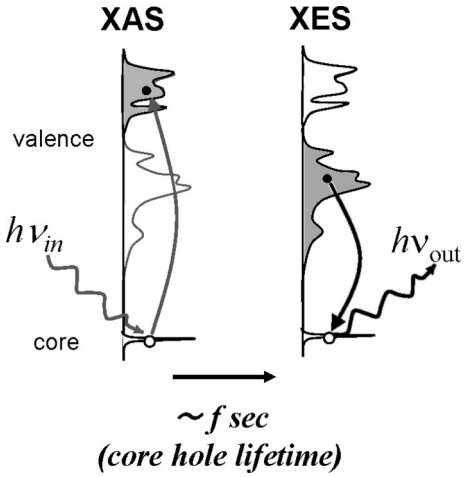

Figure 2 Schematic diagrams showing the relationship between X-ray absorption spectroscopy (XAS) and X-ray emission spectroscopy (XES).

2 X-ray emission spectroscopy Figure 2 illustrates the relationship between X-ray absorption spectroscopy (XAS) and XES. In the XAS process, absorption of incident X-ray excites an electron to empty valence state leaving a hole at the core state, providing information on unoccupied states. In the XES process, an electron in the filled valence state recombines the core hole produced by the precedent XAS and emits an X-ray photon, giving information on the occupied states [26]. Thanks to this property, XES is applicable to solids ranging from metals to wide gap insulators including $CuFeS_2$ and related materials [27, 28]. This technique has the advantage that it can probe electronic states at larger depth than the photoemission spectroscopy (PES) which can only probe electronic states near the surface.

Figure 3 shows electronic excitation processes which occur during the resonant XES associated with the L-edge of a transition metal element in a transition metal compound. The left panel describes a ground state of $3d^5$. The central panel describes an intermediate state, where a 2p core-electron is excited by X-ray irradiation to unoccupied portion of 3d states resulting in a $2p^53d^6$ configuration. The latter state is the same as the XAS final state. In the resonant XES process, the intermediate state makes a transition to the final state as described in the right panel, the 3d electron filling the core hole of the intermediate state. This process is also called "resonant inelastic X-ray scattering (RIXS)". However, in this paper we use the term resonant XES instead.

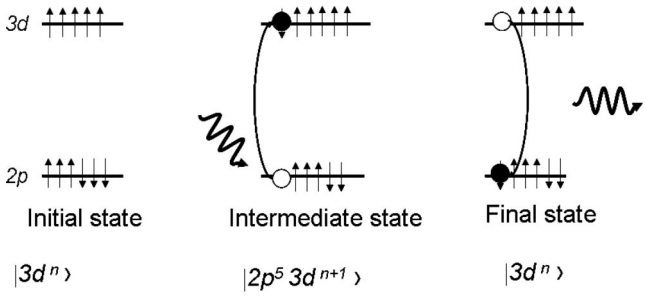

Figure 3 Electronic processes during resonant X-ray emission spectroscopy ($n = 5$).

In a resonant XES spectrum usually three kinds of peaks are observed. One is an elastic peak which appears at the same energy position as the incident X-ray energy; the second is a d–d multiplet peak characteristic of the $3d^5$ states located around the transition metal site, and the third is a CT peak peculiar to the particular compound. The d–d multiplet transitions become allowed in resonant XES, if an excited configuration in the $3d^6$ manifold is involved in the intermediate state. Such d–d transitions can be observed in resonant XES even if they cannot be observed in the ordinary optical absorption spectroscopy due to an overlap of strong CT absorptions. Therefore, the resonant XES is thought to provide a helpful tool to unravel the overlapping d–d and charge-transfer transitions extending well above the absorption edge, which cannot be observed by ordinary optical absorption spectroscopy.

3 Experiments The single crystal of chalcopyrite $CuFeS_2$ used in this experiment was grown by the Bridgman technique. The details of the growth were described in Ref. [4]. XES experiments have been carried out using synchrotron radiation beam line BL27SU at SPring-8. The spectrometer employed in this study was a specially designed flat-field-type, the details of which were described elsewhere [29]. The energy resolution of the incident and detected photons at the Fe 2p edge was 0.2 eV and 1.0 eV, respectively. Incident X-rays with two nonequivalent polarization conditions were used: vertically polarized X-rays, where the polarization vector of which are included in emitted photons, and horizontally polarized X-rays that have polarization vectors perpendicular to those in emitted photons. These polarization conditions correspond to the so-called polarized and depolarized configurations, respectively, in optical Raman spectroscopy. The polarization dependence of resonant XES provides information about local symmetry of d–d excitations. The XES spectra were measured for the energy region between 693 eV and 715 eV with the incident photon energy fixed at 710 eV, which is 2 eV above the reported position of the XAS peak [10]. The incident photon energy was tuned to the upper shoulder of the XAS peak in order to reduce overlap of the lower end of the intense elastic scattering with the d–d multiplet peaks of most interest here.

4 Results Figure 4 shows XES spectra of Fe L_3 edge in $CuFeS_2$ for horizontal and vertical polarizations. The prominent peak at 710 eV in the vertical-polarization spectrum can be assigned to an elastic peak, while a broad emission band observed for both polarizations may contain information on d–d and CT transitions, as well as fluorescence band. The fluorescence spectrum was obtained by a

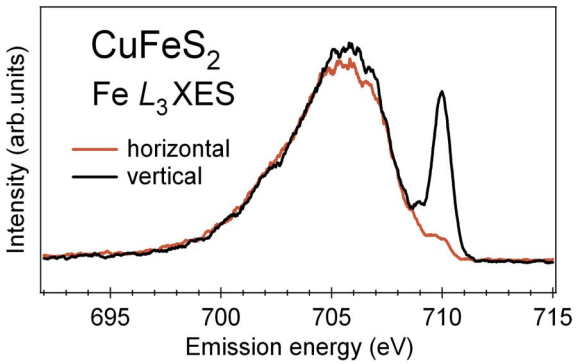

Figure 4 (online colour at: www.pss-a.com) Raw XES spectra of Fe L_3 edge in $CuFeS_2$ for horizontal and vertical polarizations.

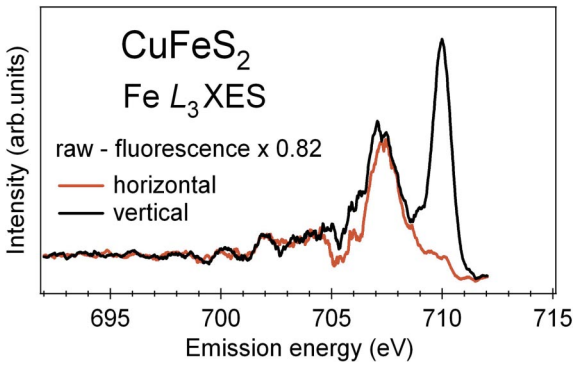

Figure 6 (online colour at: www.pss-a.com) Resonant X-ray emission spectra of Fe L_3 edge in $CuFeS_2$ obtained by subtraction of fluorescence from the raw XES data.

nonresonant XES measurement with the excitation energy of 750 eV, as shown in Fig. 5.

By subtracting the nonresonant XES (fluorescence) spectrum of Fig. 5 from the raw XES spectrum shown in Fig. 4, resonant XES spectra for two polarizations are obtained. The result of this data processing is given in Fig. 6. The fluorescence intensity was reduced to 82% so as the lower tail part of the raw data below 700 eV shown in Fig. 4 is completely wiped out by subtraction. A prominent peak appears at 707 eV for two polarizations and a small shoulder is observed at around 709 eV for vertical polarization.

5 Cluster calculations with CI If a simple ligand-field approach is employed, strongly reduced values of Racah's parameter B and C as small as 20–23% of the original value are necessary to explain the energy position of resonant XES shoulder at 709 eV, and no peaks around 706–707 eV can be predicted.

Therefore we adopted a full multiplet cluster calculation with configuration interaction (CI) in FeS_4 cluster. The method of calculation is the same as that described in Ref. [30]. The Hamiltonian assumed is given in the following:

$$
\begin{aligned}
H_{\mathrm{I}} = & \sum_{\Gamma,\sigma} \varepsilon_{3\mathrm{d}}(\Gamma)\, d^{+}_{\Gamma\sigma} d_{\Gamma\sigma} + \sum_{m,\sigma} \varepsilon_{2\mathrm{p}}\, p^{+}_{\mathrm{m}\sigma} p_{\mathrm{m}\sigma} \\
& + \sum_{\Gamma,\sigma} \varepsilon_{\mathrm{p}}(\Gamma)\, a^{+}_{\Gamma\sigma} a_{\Gamma\sigma} \\
& + \sum_{\Gamma,\sigma} V(\Gamma)\,(d^{+}_{\Gamma\sigma} a_{\Gamma\sigma} + a^{+}_{\Gamma\sigma} d_{\Gamma\sigma}) \\
& + U_{\mathrm{dd}} \sum_{(\Gamma,\sigma)\neq(\Gamma',\sigma')} d^{+}_{\Gamma\sigma} d_{\Gamma\sigma} d^{+}_{\Gamma'\sigma'} d_{\Gamma'\sigma'} \\
& - U_{\mathrm{dc}} \sum_{\Gamma,\mathrm{m}\sigma,\sigma'} d^{+}_{\Gamma\sigma} d_{\Gamma\sigma} (1 - p^{+}_{\mathrm{m}\sigma'} p_{\mathrm{m}\sigma'}) + H_{\mathrm{multiplet}} \,,
\end{aligned}
$$

where $V(\Gamma)$ denotes hybridization, U_{dd} on-site Coulomb interaction, and U_{dc} core–hole potential. The first, second and third terms express eigen energy of 3d, core 2p, and ligand p-orbitals, respectively. The fourth term denotes Fe 3d ligand charge transfer. The fifth and sixth terms are Fe3d on-site Coulomb interaction and Fe 2p–3d core–hole interaction, respectively. The term $H_{\mathrm{multiplet}}$ describes the intra-atomic multiplet coupling between Fe 3d states and that between Fe 3d and 2p states. The spin–orbit interactions for Fe 3d and 2p states are also included. The Slater integrals and the spin–orbit coupling constant are calculated by Cowan's Hartree–Fock program [31] and then the Slater integrals are rescaled by 80%. Charge transfer energy Δ is given as difference between $\varepsilon_{3\mathrm{d}}$ and ε_{p}. As ground state, linear combination of 3 configurations $3\mathrm{d}^{n}$, $3\mathrm{d}^{n+1}\underline{\mathrm{L}}$ and $3\mathrm{d}^{n+2}\underline{\mathrm{L}}^{2}$ is assumed. We used the following parameters: $U_{\mathrm{dd}} = 3.2$, $\Delta = -3.0$, $U_{\mathrm{dc}} = 4.0$, $V(e_{\mathrm{g}}) = 2.07$, $V(\mathrm{t2_g}) = -1.07$, in units of eV. The ground state character is $3\mathrm{d}^{5} = 22.1\%$, $3\mathrm{d}^{6}\underline{\mathrm{L}} = 54.6\%$, and $3\mathrm{d}^{7}\underline{\mathrm{L}}^{2} = 23.3\%$.

The result of calculation, which gives the best fit to experimental data, is illustrated in Fig. 7, together with the experimental spectra reproduced from Fig. 6. The charge transfer energy Δ that provides the best fit was determined as -3.0 eV. The absolute value of Δ seems rather large compared with the one obtained by the previous PES experiment [24], i.e., $\Delta = -0.5$ eV. We are confident that the value of the present study is more reliable than the

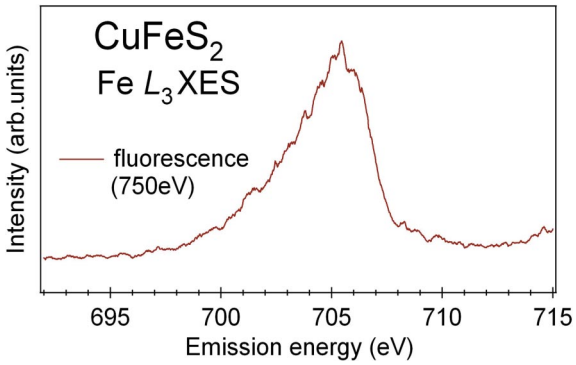

Figure 5 (online colour at: www.pss-a.com) Nonresonant XES spectrum of the Fe L_3 edge in $CuFeS_2$ measured with 750 eV X-ray excitation.

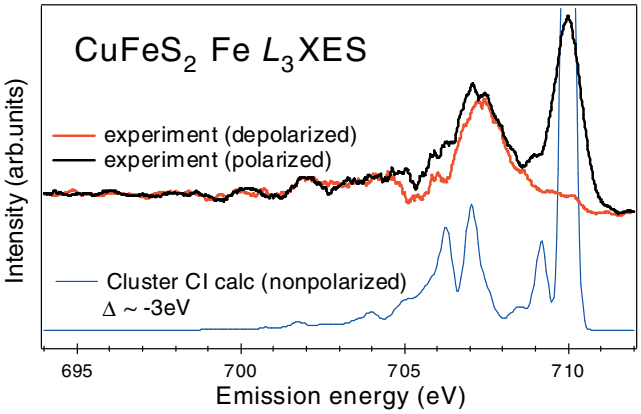

Figure 7 (online colour at: www.pss-a.com) Comparison of the XES spectrum calculated by cluster CI calculation and experimental XES of Fe L_3 edge in $CuFeS_2$.

previous one, since the latter is deduced from the theoretical fit to the spectrum with poor resolution.

The observed XES peaks at 709 eV and 708.5 eV which are located around 1 eV below the elastic peak may be interpreted to be originated from the spin-allowed CT transitions between $^6A_1$ and $^6T_2$. This is consistent with the interpretation of observed optical absorption peaks described in Section 1.

The problems of the electronic states of Fe in $CuFeS_2$ gives much insight to the electronic states of Fe in hemoprotein, since a negative or very small value of Δ is also found in the latter [32], which results in interesting physical properties such as the spin cross-over phenomenon in the multiple valence state of transition metal.

6 Conclusion Resonant X-ray emission spectroscopy has been carried out on Fe L_3 edge of $CuFeS_2$. The experimental spectrum was compared with theoretical one obtained by cluster CI calculation, from which it is found that the previous assignments of the optical absorption are consistent with that of resonant XES.

The spectral details are successfully explained by assuming that the charge transfer energy Δ takes a negative value. This result is consistent with the previous consideration that $CuFeS_2$ is a Haldane–Anderson type insulator. The strong hybridization is found to be a dominant cause of the mysterious 3d electron behaviours in this material.

Acknowledgements This work was partially supported by a Grant-in-Aid for Scientific Research from MEXT in Priority Area "Creation and Control of Spin Current" (19048012) and a Grant-in-Aid for Scientific Research from JSPS (16104004). Authors are very grateful to Prof. S. Sugano for valuable suggestions and enlightening discussions on this problem.

References

[1] B. I. Boltaks and N. N. Tarnovskii, Zh. Tekh. Fiz. **25**, 402 (1955).
[2] T. Teranishi, J. Phys. Soc. Jpn. **16**, 1881 (1961).
[3] T. Teranishi, K. Sato, and K. Kondo, J. Phys. Soc. Jpn. **36**, 1618 (1974).
[4] T. Teranishi and K. Sato, J. Phys. (Paris) **36**, C3-149 (1975).
[5] G. Donnay, L. M. Corliss, J. D. H. Donnay, N. Elliot, and J. M. Hastings, Phys. Rev. **112**, 1917–1923 (1958).
[6] L. Pauling and L. O. Brockway, Z. Kristallogr. **82**, 188 (1932).
[7] E. Frank, Nuovo Cimento B **63**, 407 (1968).
[8] D. Raj, K. Chandra, and S. P. Puri, J. Phys. Soc. Jpn. **24**, 39 (1968).
[9] J. Schneider, A. Rauber, and G. Brandt, J. Phys. Chem. Solids **34**, 443 (1973).
[10] Yu. Mikhlin, Ye. Tomashevich, V. Tauson, D. Vyalikh, S. L. Molodtsov, and R. Szargan, J. Electron. Spectrosc. Relat. Phenom. **142**, 83 (2005).
[11] S. W. Goh, A. N. Buckley, R. N. Lamb, R. A. Rosenberg, and D. Moran, Geochim. Cosmochim. Acta **70**, 2210 (2006).
[12] C. I. Pearce, R. A. D. Pattrick, D. J. Vaughan, C. M. B. Henderson, and G. van der Laan, Geochim. Cosmochim. Acta **70**, 4635 (2006).
[13] I. G. Austin, C. H. L. Goodman, and A. E. Pengelly, J. Electrochem. Soc. **103**, 609 (1956).
[14] K. Sato and T. Teranishi, J. Phys. Soc. Jpn. **40**, 297 (1976).
[15] T. Oguchi, K. Sato, and T. Teranishi, J. Phys. Soc. Jpn. **48**, 123 (1980).
[16] T. Kambara, J. Phys. Soc. Jpn. **36**, 1625 (1974).
[17] T. Hamajima, T. Kambara, and K. I. Gondaira, Phys. Rev. B **24**, 3349 (1981).
[18] K. Sato and T. Teranishi, J. Phys. Soc. Jpn. **37**, 415 (1974).
[19] K. Sato, K. Tanaka, K. Ishii, and S. Matsuda, J. Cryst. Growth **99**, 772 (1990).
[20] X.-J. Li, Y. Kudo, S. Matsuda, I. Aksenov, and K. Sato, Jpn. J. Appl. Phys. **31**, L303 (1992).
[21] S. Sugano, Y. Tanabe, and H. Kamimura, Multiplets of Transition-Metal Ions in Crystals (Academic Press, New York, 1970).
[22] T. Kambara, K. Suzuki, and K. I. Gondaira, J. Phys. Soc. Jpn. **39**, 764 (1975).
[23] F. D. M. Haldane and P. W. Anderson, Phys. Rev. B **13**, 2553 (1976).
[24] M. Fujisawa, S. Suga, T. Mizoguchi, A. Fujimori, and K. Sato, Phys. Rev. B **49**, 7155 (1994).
[25] J. Zaanen, G. A. Sawatzky, and J. W. Allen, Phys. Rev. Lett. **55**, 418 (1985).
[26] A. Kotani and S. Shin, Rev. Mod. Phys. **73**, 203 (2001).
[27] E. Z. Kurmaev, J. van Ek, D. L. Ederer, L. Zhou, T. A. Callcott, R. C. C. Perera, V. M. Cherkashenko, S. N. Shamin, V. A. Trofimova, S. Bartkowski, M. Neumann, A. Fujimori, and V. P. Moloshag, J. Phys.: Condens. Matter **10**, 1687 (1998).
[28] K. C. Prince and M. Matteucci, Phys. Rev. B **71**, 085102 (2005).
[29] T. Tokushima, Y. Harada, H. Ohashi, Y. Senba, and S. Shin, Rev. Sci. Instrum. **77**, 063107 (2006).
[30] M. Taguchi, P. Krüger, J. C. Parlchas, and A. Kotani, Phys. Rev. B **73**, 125404 (2006).
[31] R. D. Cowan, The Theory of Atomic Structure and Spectra (University of California Press, Berkeley, 1981).
[32] Y. Harada, M. Taguchi, Y. Miyajima, T. Tokushima, Y. Horikawa, A. Chainani, Y. Shiro, Y. Senba, H. Ohashi, H. Fukuyama, and S. Shin, J. Phys. Soc. Jpn. **78** (2009), in press.

